Biochimica et Biophysica Acta 1853 (2015) 1646–1657

Contents lists available at ScienceDirect

Biochimica et Biophysica Acta

journal homepage: www.elsevier.com/locate/bbamcr

mTor mediates tau localization and secretion: Implication for Alzheimer's disease☆

Zhi Tang [a,b], Eniko Ioja [a], Erika Bereczki [a], Kjell Hultenby [c,1], Chunxia Li [a], Zhizhong Guan [a,d,e], Bengt Winblad [a], Jin-Jing Pei [a,f,g,*]

[a] Karolinska Institutet, NVS Department, Centrum for Alzheimer Research, Division for Neurogeriatrics, Novum, SE 14186 Stockholm, Sweden
[b] Department of Clinical Laboratory, Guizhou Provincial People's Hospital, Guiyang, Guizhou, China
[c] Clinical Research Center, Department of Laboratory Medicine, Karolinska Institutet, Karolinska University Hospital Huddinge, SE 141 86 Stockholm, Sweden
[d] Department of Pathology, Guiyang Medical College, Guiyang 550004, Guizhou, China
[e] Molecular Biology, Guiyang Medical College, Guiyang 550004, Guizhou, China
[f] Department of Neurology, Xuan Wu Hospital, Capital Medical University, China
[g] Center of Alzheimer's Disease, Beijing Institute for Brain Disorders, Beijing 100053, China

ARTICLE INFO

Article history:
Received 23 September 2014
Received in revised form 23 February 2015
Accepted 3 March 2015
Available online 17 March 2015

Keywords:
mTor
Tau secretion
Autophagy
Tau phosphorylation
Alzheimer's disease

ABSTRACT

Abnormally hyperphosphorylated tau aggregates form paired helical filaments (PHFs) in neurofibrillary tangles, a key hallmark of Alzheimer's disease (AD) and other tauopathies. The cerebrospinal fluid (CSF) levels of soluble total tau and phospho-tau from clinically diagnosed AD patients are significantly higher compared with controls. Data from both *in vitro* and *in vivo* AD models have implied that an aberrant increase of mammalian target of rapamycin (mTor) signaling may be a causative factor for the formation of abnormally hyperphosphorylated tau. In the present study, we showed that in post-mortem human AD brain, tau was localized within different organelles (autophagic vacuoles, endoplasmic reticulum, Golgi complexes, and mitochondria). In human SH-SY5Y neuroblastoma cells stably carrying different genetic variants of mTor, we found a common link between the synthesis and distribution of intracellular tau. mTor overexpression or the lack of its expression was responsible for the altered balance of phosphorylated (p-)/-non phosphorylated (Np-) tau in the cytoplasm and different cellular compartments, which might facilitate tau deposition. Up-regulated mTor activity resulted in a significant increase in the amount of cytosolic tau as well as its re-localization to exocytotic vesicles that were not associated with exosomes. These results have implicated that mTor is involved in regulating tau distribution in subcellular organelles and in the initiation of tau secretion from cells to extracellular space.

1. Introduction

Alzheimer's disease (AD), the most common age-related neurodegenerative disorder is characterized by the presence of neurofibrillary tangles (NFTs), senile plaques (SP) and progressive neurodegeneration [1]. In AD, the severity of dementia has been positively related to the degree of NFT deposition [2]. NFTs are intraneuronal inclusions that are composed of straight and paired helical filaments (PHFs), the major component of which is the aberrantly hyperphosphorylated form of the microtubule-associated protein tau [3,4]. Such abnormal filaments accumulate in the cell bodies of diseased but surviving neurons, as well as in the dystrophic neurites, and neuropil threads in and around SPs [5,6]. Regulation of microtubule assembly and stabilization is the most studied function of tau, although it is becoming convincingly evident that tau might play an additional role in the cell. In addition to phosphorylation other site specific posttranslational modifications, such as glycosylation or O-GlcNAcylation occur to tau [7]. The functions of tau are regulated by site-specific phosphorylation, carefully coordinated by kinases and phosphatases, which if dysregulated, in various disease state, result in tau dysfunction and re-localization [6], potentially followed by tau aggregation, neuronal and synaptic dysfunction and ultimately cell death. In AD, studies on postmortem brain tissues show a progressive spread of tau deposits from the transentorhinal cortex to the hippocampus, that eventually spreads to most cortical areas [8]. A

☆ This work was supported by Karolinska Institutet Research funds, Dementia Foundation, Alzheimerfonden, Wallenberg foundation, Gun and Bertil Stohnes Foundation, Gamla Tjanarinnor Foundation, Karolinska Institutet Strategic Neuroscience Program, Swedish Brain Power Programme and Sheikha Salama Bint Hamdan Al Nahyan Foundation.

* Corresponding author at: Karolinska Institutet, NVS Department, Centrum for Alzheimer Research, Division for Neurogeriatrics, Novum, Floor 5, 14157 Stockholm, Sweden. Tel.: +46 8 58583639; fax: +46 8 58583880.
E-mail address: Jin-Jing.Pei@ki.se (J.-J. Pei).
[1] Clinical Research Center, Department of Laboratory Medicine, Karolinska Institutet, Karolinska University Hospital Huddinge, SE 141 57 Stockholm, Sweden.

http://dx.doi.org/10.1016/j.bbamcr.2015.03.003
0167-4889/

similar spreading pattern has also been described in other tauopathies [9]. Besides interacting with microtubules, tau also interacts with neuronal membranes, such as plasma membrane [10], endoplasmic reticulum (ER) [11], and Golgi apparatus [12], where part of the posttranslational modifications occur. Regarding its localization, tau is mainly localized in the axons of neuronal cells but can also be found in the nucleus, dendrites and synapses. However, intracellular localization of tau in *in vitro* and *in vivo* AD models and its underlying mechanism is still poorly understood. In addition, an inverse relationship has been established in damaged areas between the number of extracellular NFT (ghost tangles) and the number of surviving neurons [13,14]. The CSF levels of total soluble tau and p-tau from clinical AD patients are significantly higher compared with control cases [15,16]. The released extracellular tau also aggregates in AD brain, being possibly toxic for the surrounding neurons [17,18]. Recent studies report that extracellular tau is detected in different cellular systems and mouse models with or without overexpressing tau [19].

Both, *in vitro* and *in vivo*, tau is a substrate for several kinases. The co-localization of NFTs with some kinases such as glycogen synthase kinase-3β (GSK-3β), mitogen-activated protein kinase (MAPK), microtubule affinity-regulating kinase (MARK), p70S6 kinase (p70S6K), and protein kinase B (PKB) [20–23] has been already proven although other kinases might co-localize with tau as well. The mammalian target of rapamycin (mTor) is a 289-kDa serine/threonine kinase, which consists of two multiprotein complexes known as mTor complex mTorC1 and mTorC2 [24]. mTorC1 controls cellular homeostasis *via* activating p70S6 kinase (S6K), and being inhibited by rapamycin. In contrast mTorC2 is insensitive to rapamycin and controls cell survival *via* PI3K and phosphoinositide-dependent kinase (PDK) 2 pathway [25].

mTor plays an important role in protein homeostasis. We have found mTor being co-localized with NFTs and mediating tau phosphorylation at S214, S356 and T231 *in vitro*, as well as that mTor mediates the synthesis and aggregation of tau, resulting in compromised microtubule stability [26–28]. mTor is also an inhibitor of macroautophagy, a conserved intracellular system designed for the degradation of long-lived proteins and organelles in lysosomes [29]. Macroautophagy is induced when an isolation membrane is generated surrounding cytosolic components forming an autophagic vacuole (AVs) which will eventually fuse with lysosomes for protein/organelle degradation. The induction of autophagosome is negatively regulated by mTor [30]. Sixteen autophagy-related proteins (Atg) are involved in different stages of the autophagic processes [31]. LC3 (microtubule associated protein light chain 3) is the homologue of Atg8 in yeast that participates in the formation of autophagosomal membrane. After its synthesis, LC3 is cleaved by Atg4 to form LC3-I being further converted to LC3-II by Atg7 and Atg3 [32]. LC3-II a lipid conjugate that localizes to autophagosome membrane is often used as a marker of ongoing autophagy. Cumulative evidence suggests that an age-dependent decrease in the autophagy/lysosome system may account for the accumulation of abnormal proteins during aging [33]. AVs are rare in neurons of normal adult brains [34]. In AD brains AVs appear in neocortical and hippocampal pyramidal neurons and accumulate markedly within the dendritic arbors of these affected cells [34].

The intraneuronal distribution of tau protein and the mechanisms behind mTor-tau interactions consequently leading to tau hyperphosphorylation and aggregation in AD represents a topic of increasing interest. It is not clear how and whether mTor influences secretion of tau to extracellular space. In this article our main purpose was to study the relationship between tau protein in various cellular compartments responsible for protein synthesis and secretion (such as ER, Golgi apparatus and mitochondria) and the autophagosomes in relationship to mTor activity. In order to investigate the link between mTor and tau trafficking, in the present study we have compared AD and control human brain samples, as well as a series of human SH-SY5Y neuroblastoma cells carrying a series of genetic modifications of mTor.

2. Experimental procedures

2.1. Antibodies, reagents and materials

Detailed information regarding the antibodies used in the study, are presented in Table 1. Okadaic acid, protease inhibitor cocktail, alkaline phosphatase (AP), trichloroacetic acid, and acetone were purchased from Sigma-Aldrich Sweden AB (Stockholm, Sweden), culture media from Invitrogen (Stockholm, Sweden), bicinchoninic acid (BCA) kit from Pierce (Stockholm, Sweden), while Immobilon Western chemiluminescent HRP Substrate from Millipore (Stockholm, Sweden).

2.2. Cell cultures

We have reported the establishment of a series of stable SH-SY5Y cell lines that carry a selection of constructs expressing: empty pcDNA3.0 plasmids (V1) and pcDNA3.0 plasmids with human flag-mTor wild type (m-WT), human flag-mTor-S2035T (rapamycin resistant site, m-S), and human flag-mTor-S2035T/D2357E (both rapamycin resistant and kinase dead sites, m-SD) constructs as well as stable cell lines that carry empty vector pLko.1 (V2) (0.5 μg/ml puromycin), or pLko.1 with suppression of mTor expression (m-SR1 and m-SR2). Cell lines that carry both empty pcDNA3.0 vector and EECMV plasmids (V3), and both pcDNA3.0 vector and EECMV plasmids with S6K kinase dead (S6K-KD) were also established [26]. Briefly, the SH-SY5Y cells were grown to 70–80% confluence in 100 mm culture dishes in Dulbecco's modified Eagle's medium (DMEM)/F12 medium (1:1) supplemented with 10% fetal bovine serum (FBS) (Invitrogen, Stockholm, Sweden). In order to induce autophagic activity and minimize cell death responses, cells were induced by serum deprivation in 2 steps: first, cells were cultured in DMEM/F12 with 1% FBS for 24 h, then kept in serum free medium for 4.5 h.

2.3. Cell fractionation

After 4.5 h serum deprivation, cells were washed with PBS and suspended in Triton lysis buffer (1% Triton X-100 in 50 mM Tris, 150 mM NaCl, pH 7.4) containing protease and phosphatase inhibitors 2 mM EGTA, 25 mM NaF, 200 μM Na3VO4, 0.5 mM phenylmethylsulfonyl fluoride (PMSF), 5 mM EDTA, 1 μM okadaic acid, and protease inhibitor cocktail (1:200). Cell lysates were sonicated on ice and centrifuged in two steps: 1) at 1000 ×*g*, 4 °C for 10 min to collect supernatants free of nuclei and cell debris; 2) at 100,000 ×*g*, 4 °C for 1 h for separating supernatant (cytosolic fraction) from pellet (microsomal membrane fraction) re-suspended in the same Triton lysis buffer.

2.4. Isolation of endoplasmic reticulum, mitochondria and Golgi membrane fractions

Cellular fractions were prepared according to a method described by Bozidis with small modifications [35]. After serum deprivation, cells were harvested by centrifugation at 1400×*g* for 5 min; suspended in mannitol/Tris/EDTA (MTE) buffer containing 270 mM D-mannitol, protease and phosphatase inhibitors — 2 mM EGTA, 5 mM EDTA, 25 mM NaF, 1 mM Na3VO4, 1 μM okadaic acid and protease inhibitor cocktail (Sigma) (1: 200), and then sonicated 3 × 10 s. Crude ER and mitochondria were separated by centrifugation of cell lysates for 10 min at 15,000 ×*g* at 4 °C. Supernatant containing crude ER was layered on top of a sucrose gradient (2 M, 1.5 M and 1.3 M sucrose) and centrifuged for 70 min at 152,000 ×*g*, 4 °C. ER fractions were collected at the interface of 1.3 M sucrose gradient using a 20-G needle then washed with 1 × MTE buffer and centrifuged at 126,000 ×*g* for 45 min at 4 °C. The final ER pellets were resuspended in Triton lysis buffer. Crude mitochondrial pellets were gently washed and resuspended in 1 × MTE buffer then layered on a mitochondrial sucrose gradient (1.7 M and 1.0 M

Table 1
Antibodies used in this study. Abbreviations used are as follows: T—total, r—rabbit, m—mouse, p—phosphorylated, de-p—dephosphorylated, IF—immunofluorescence, WB—Western blot, DB—dot blot.

Antibody	Host	Specificity	Phospho-epitopes	WB/DB dilution	IF dilution	Sources
Anti-Raptor (24C12)	r	T raptor	–		1:100	Cell signaling
Anti-LC3B	r	N-terminal LC3-B	–		1:3000	Novus biologicals
Anti-LC3-5F10	r	N-terminal LC3-B	–	1:400	1:100	Nanotools
Anti-Rab5	m	Early endosome and plasma membranes	–	1:400		BD transduction laboratories™
Anti-lamp1	m	Lysosomal membrane proteins1	–	1:400	–	BD transduction laboratories™
Tau-1	m	De-p tau	S198/199/202/205	1:80,000	1:40,000	Dr I. Binder, USA
PHF-1	m	p-Tau	S396/404	1:400	1:400	Dr P. Davies, USA
TG3	m	p-Tau	T231/S235	1:40	1:20	Dr P. Davies, USA
R134d	r	T tau	–	1:5000	1:500	Dr K. Iqbal, USA
DC190 (anti-pan tau)	m	T tau		1:5000	1:500	Dr. M Novak, Slovakia
AT8	m	p-Tau	S202/T205		1:500	Innogenetics
Anti-Tau S214	r	p-Tau	S214	1:1000	1:100	Invitrogen
Anti-Tau S422	r	p-Tau	S422	–	1:1000–6000	Invitrogen
Golgin 97	m	Golgi marker			1:500	Molecular probes
Syntaxin 6 (C34B2)	r	Golgi marker		1:1000	1:100	Cell signaling
COX IV (3E11)	r	Mitochondrial marked		1:1000	1:125	Cell signaling
KDEL (10C3)	m	ER marker		1:1000		Enzo life science
Anti-mTor (7C10)	r	T mTor	–	1:10,000	–	Cell signaling
Anti-p-mTor	r	P, active mTor	S2448	1:1000	1:100	Cell signaling
Anti-S6K (49D7)	r	T S6K	–	1:1000	–	Cell signaling
Anti-p-S6K (108D2)	r	P, active S6K	T389	1:1000	1:100	Cell signaling

sucrose) and centrifuged 22 min at 40,000 ×*g*, 4 °C. Mitochondrial fraction was collected from the interface of 1.7 M and 1.0 M sucrose gradient then washed and centrifuged at 15,000 ×*g* for 10 min at 4 °C. Final pellets were resuspended in Triton lysis buffer.

For the separation of Golgi fraction cells were homogenized in a Dounce homogenizer using 10 – 15 strokes [36]. Homogenates were brought to 1.4 M sucrose solution by adding two volumes of 2.0 M sucrose then layered on the top of 1.6 M sucrose solution, overlaid with 1.2 M and 0.8 M sucrose gradient solutions. Gradients were centrifuged at 110,000 ×*g* for 2 h at 4 °C. Golgi fraction was collected at the 0.8 M/1.2 M sucrose interface then washed and centrifuged at 100,000 ×*g* for 30 min at 4 °C. Final pellet was resuspended in Triton lysis buffer.

2.5. Exosome isolation

Exosomes were prepared from supernatants of cell culture media [37]. Media was collected after 4.5 h serum deprivation and sequentially centrifuged at 300 ×*g*, 4 °C for 10 min, 2000 ×*g*, 4 °C for 10 min, and 10,000 ×*g*, 4 °C for 30 min to remove cells and cell debris, then spun again at 100,000 ×*g*, 4 °C for 2 h to obtain crude exosomes pellets. Pellets were resuspended in PBS, centrifuged at 100,000 ×*g*, 4 °C for 1 h to separate exosomes. Collected exosomes were suspended in 1% Triton X-100 lysis buffer.

2.6. Protein purification and isolation from conditioned culture media

Cell culture media supernatants were collected after serum deprivation for 4.5 h and sequentially centrifuged at 300 ×*g*, 4 °C for 10 min, 2000 ×*g*, 4 °C for 10 min, and 10,000 ×*g*, 4 °C for 30 min to remove cells and cell debris. The supernatant was collected, added with ice-cold 100% trichloroacetic acid [38] (1:8), vortexed and incubated at 4 °C for 2 h. The samples were centrifuged at 20,000 ×*g* at 4 °C for 30 min and the supernatants were carefully aspirated. 1 ml 100% ice-cold acetone was added to the pellets which were briefly vortexed and incubated at −20 °C for 1 h. The samples were centrifuged at 20,000 ×*g* at 4 °C for 30 min and the pellets were washed twice with 100% ice-cold acetone. The final pellets were allowed to air dry at 23 °C [39] then were suspended in 1% Triton X-100 lysis buffer.

2.7. Immunohistochemistry and immunofluorescence

Brain tissues from 6 AD cases and 6 age-matched non-neurological controls from The Netherlands Brain Bank were used in the study (Table 2). As described in our previous paper [26], paraffin sections (6 μm) of the hippocampus and adjacent temporal cortex were deparafinized in xylene, rehydrated with different gradient ethanol (100%–95%–70%), and blocked with buffer containing 5% bovine serum albumin (BSA, Sigma) and 0.1% Triton X-100 in TBS for 1 h followed by an incubation with various primary antibodies. The bound autophagosome marker LC3 antibodies were incubated with secondary anti-mouse and detected using the avidin-biotin system from Vectastain (BioNordika AB, Stockholm, Sweden), and visualized with 3, 3′-diaminogenizidine (DAB) (Sigma-Aldrich Sweden AB, Stockholm, Sweden) as brown color [26]. The sections were subsequently incubated with tau (PHF-1, p-tau Ser(P)-422), or Aβ 6E10 antibodies, and visualized by Vector® SG (BioNordika AB, Stockholm, Sweden) as dark gray/blue color. Control sections were used in order to control for unspecific signals.

For immunofluorescent staining, sections were incubated with primary antibodies against KDEL, COX IV or Golgin 97 and anti-p-tau (R134d, p-tau Ser(P)-422, PHF-1 and AT8) overnight at 4 °C. Following

Table 2
Human material case details. Abbreviations used are as follows AD—Alzheimer disease, Control—non-demented control, f—female, m—male, PMD—post-mortem delay, Br.wt—Brain weight (g)., Br. Staging—Neurofibrillary staging criteria by Braak & Braak.

Case nr	Diagnosis	Gender	Age	PMD (hour:minute)	Br.wt	ApoE (allele)	Br. Staging
1	AD	F	54	03:55	1089	33	6
2	AD	F	74	04:30	1070	43	6
3	AD	F	78	03:10	1019	43	5
4	AD	F	87	06:55	1010	43	5
5	AD	M	62	03:30	1287	43	5
6	AD	M	83	03:15	1315	33	6
7	Control	F	55	05:35	1363	43	0
8	Control	F	73	04:40	1360	32	0
9	Control	M	51	07:44	1550	33	0
10	Control	M	62	09:35	1175	33	0
11	Control	M	71	07:40	1190	33	1
12	Control	M	83	08:50	1120	33	1

treatment, cells plated on coverslips were rinsed with buffer (pH 6.85) containing 80 mM HEPES, 10 mM EGTA and 2 mM MgCl2 (HEM) and then fixed in 4% paraformaldehyde/HEM buffer (1: 1) for 30 min. Cells were permeated with Tris-buffered saline (TBS) containing 0.1% Triton X-100 for 5 min. For staining with the Tau-1 antibody, cells were permeabilized in the presence of 30% glycerol and dephosphorylated with alkaline phosphatase (149 U/ml) in 100 mM Tris, pH 8.0 at 37 °C for 6 h [40], then washed three times with TBS buffer. Unspecific binding sites were blocked with buffer containing 5% BSA and 0.1% Triton X-100 in TBS for 30 min. Cells were incubated with primary antibodies against KDEL, COX IV or Golgin 97, Raptor, LC3, R134d, p-tau Ser(P)-422, p-tau Ser(P)-214, Tau-1, PHF-1 and TG3 overnight at 4 °C. Unbound antibody for both brain sections and cell staining was removed by washing. Bound antibody was detected by incubation for 1 h with Dylight 488 conjugated goat anti-mouse IgGs or Dylight 594 conjugated goat anti rabbit IgGs (1:200 for both, JACKSON ImmunoResearch). After staining the nuclei with DAPI, fluorescent signals were assessed using confocal microscopy (Zeiss, Oberkochen, Germany).

2.8. Immunoelectron microscopy (EM)

After serum deprivation for 4,5 h cells were fixed in 3% paraformaldehyde in 0.1 M phosphate buffer (PB), pH 7.4. Cells were then infiltrated with 10% gelatin in 0.1 M PB and fixed in the same fixative as above. Small pieces were cut and then infiltrated with 2.3 M sucrose and frozen in liquid nitrogen. Sectioning was performed according to Tokuyasu [41] at −95 °C. To block non-specific binding the sections were placed on drops of 2% normal goat serum in 0.1 M PB (PBG) pH 7.4 for 2 h. Subsequently the sections were incubated with the primary mouse anti-Tau 1 antibody diluted 1:100 in PBG overnight in a humidified chamber. The sections were thoroughly washed in PBS buffer, and bound antibodies were detected with secondary goat anti mouse antibodies conjugated to 10 nm gold nanoparticles (Biocell, BBInternational, Cardiff, England), diluted 1:100 in PBG. Sections were then washed, and embedded in 1% methyl cellulose containing 0.02% uranyl acetate. Grids were analyzed in a Tecnai 12 Bio TWIN (FEI Company, Eindhoven, The Netherland) and images were taken using a Veleta camera (Soft Imaging System, GmbH, Muenster, Germany) [42].

2.9. Western and dot blotting

Protein concentration of samples prepared from the stable cell lines was determined by a bicinchoninic acid (BCA) kit (Pierce, Rockford, IL, USA). In the case of Western blotting equal amounts (20–80 μg/lane) of protein were loaded onto 8–12.5% (w/v) SDS-polyacrylamide gels. Separated proteins were blotted onto PVDF membranes (MILLIPORE AB, Solna, Sweden). For dot blots equal amounts (3–5 μg/dot) of protein sample from cell homogenates or conditioned culture media fractions were dotted onto a nitrocellulose membrane. The protein on the membrane was permeabilized in the presence of 30% glycerol and dephosphorylated with alkaline phosphatase (149 U/ml) in 100 mM Tris, pH 8.0 at 37 °C for 18 h [40] to analyze tau phosphorylation at S198/199/202/205 sites by Tau-1 antibody. Membranes were blocked in 5% (w/v) nonfat milk for 1 h diluted in Tris-buffered saline supplemented with 0.1% (v/v) Tween-20 (TBST) followed by an incubation with primary antibodies (Table 1) at 4 °C overnight, and then with secondary peroxidase coupled anti-mouse or anti-rabbit antibodies (1:2000, GE Healthcare AB, Solna, Sweden) at room temperature for 1 h. After exposure to Hyperfilm MP (Amersham Biosciences) intensities were analyzed using Image J software. Probed filters were stripped by using stripping buffer (100 mM 2-Mercaptoethanol, 2% SDS, 62.5 mM, Tris–HCl pH 6.8) at 50 °C for 30 min.

2.10. Statistical analysis

Statistical comparisons between different experimental groups were performed by one-way ANOVA followed by Bonferroni post-hoc test analyses. A value of $p \leq 0.05$ was considered as significant.

3. Results

3.1. Coexistence of tau deposits in tangle-bearing neurons with clustered autophagic vacuoles, endoplasmic reticulum, mitochondria and Golgi apparatus in AD brains

We have used double immunostaining with the autophagy marker light chain LC3 (and II) and tau (PHF-1 or anti-Ser(P)-422) or amyloid beta (Aβ) (6E10) antibodies to identify the coexistence of AVs with tau or amyloid pathology. The control human brains presented negligible tau pathology displaying little amount of LC3-positive cells that were mostly found in the soma of neurons (Fig. 1, A1, B1 and C1). AD brains however presented wide spread mottled immuno-clusters of LC3 (brown) co-existing with deposits positive for anti-Ser(P)-422 (blue, Fig. 1, A2–3) and PHF-1 (blue, Fig. 1, B2–3) in pyramidal tangle-bearing neurons from hippocampal CA1 region. We have observed LC3-positive stainings (brown) in the close vicinity of the core of senile plaques (blue, Fig. 1, C2 and C3) in AD brains, suggesting a partial overlap of LC3-positive cells with senile plaques.

Next we questioned whether there is difference in the localization of tau (total tau or PHF-1 or AT8 or anti-Ser(P)-422) in various cellular organelles between AD and control brain sections. We have used ER marker KDEL, Golgi apparatus marker Golgin 97, as well as the mitochondria marker COX IV. No significant difference in the immunostaining of the various organelle markers has been found between AD and control brains. Deposits of total tau (R134d) and hyper-p-tau (anti-Ser(P)-422) were observed to be partially overlapped with the ER (Fig. 1, D1 and E1), as well as with the Golgi apparatus (Fig. 1, F1 and G1) and the mitochondria (Fig. 1, H1 and I1) in the majority of neurons from AD brains. In control brains we have seen little or no hyper-phosphorylated tau pathology (Fig. 1 D2–I2), while total tau was less partially overlapped to the ER marker and Golgi marker, KDEL or Golgin 97 to similar extent as in AD brains (Fig. 1, D2 and F2).

3.2. mTor activity interferes with tau in membrane and cytosolic fractions

In the present study, we employed a series of genetically modified mTor expressing cell lines recently characterized by us [26] to analyze the levels of tau protein in membrane and cytosolic fractions from these cell lines. In the microsomal membrane fraction from up-regulated wild type mTor (m-WT) cells the levels of Np-tau (Tau-1) and total tau (R134d) were higher, while in the cytosolic fraction the levels of total tau and p-Tau (PHF-1 and TG3) were increased compared with the fraction deriving from control cells (V1), mutated mTor cells at rapamycin resistant site (m-S) and kinase dead mTor (m-SD) cells (Fig. 2, B1). In fractions prepared from cells with down-regulated mTor activity (m-SR1 and m-SR2), total and Np-tau levels were reduced in membrane fractions compared to control cells containing empty vector (V2), cytosolic p-Tau also showed decreased levels compared to control V2 cells (Fig. 2, B2). No immunoreactivity could be detected for Np-tau in the cytosolic fractions and for p-Tau species in the membrane fractions. S6 kinase dead (S6K-KD) cells have resulted in decreased levels of total tau (R134d) in both membrane and cytosolic fractions compared to control cells containing empty vector (V3). Np-tau (Tau-1) showed a decreased reactivity in membrane fraction of S6K-KD compared to V3 cells while decreased levels of p-Tau (PHF-1 and TG3) were also found in cytosolic fraction compared to V3 empty vector (Fig. 2, B3).

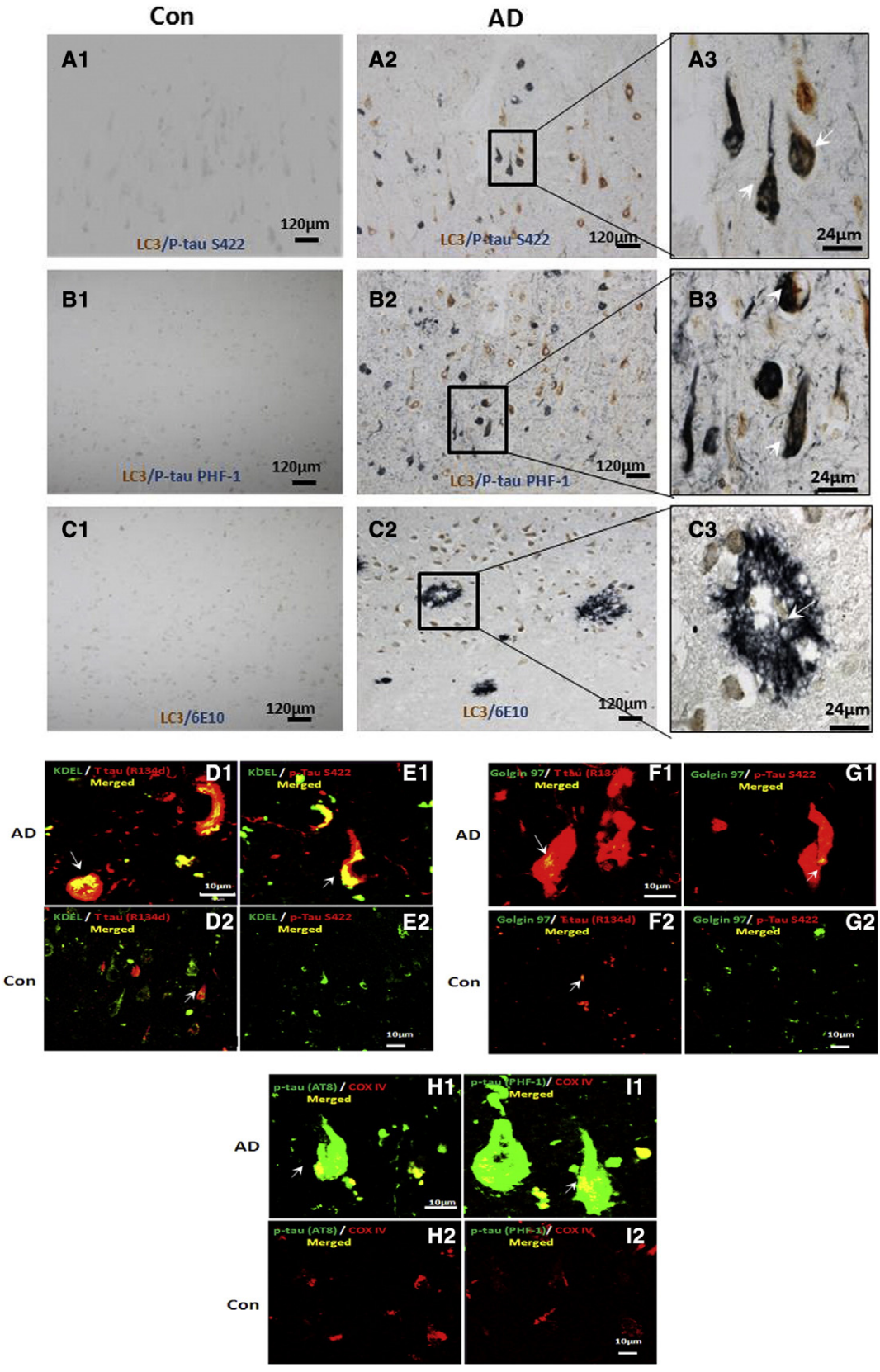

Fig. 1. Increased macroautophagy and tau accumulation in subcellular compartments of human AD and control brain. Double immunostaining for LC3 (brown), p-Tau (p-tau Ser(P)-422 and PHF-1) (A1–B3, gray/blue) and 6E10 (C1–C3, gray/blue) in CA1 pyramidal neurons of control (A1, B1, C1) and AD hippocampus (A2–3, B2–3, C2–3). In the pre-tangle and classic tangle-bearing neurons, the granular staining of KDEL (endoplasmic reticulum marker) (D1–2 and E1–2, green), Golgin 97 (Golgi apparatus marker) (F1–2 and G1–2, green) and COX IV (mitochondria marker) (H1–2 and I1–2, red) are partially overlapped with dotted or fine filamentous structures labeled by T-tau (D1 and F1, red), anti-p-Tau (p-Tau Ser(P)-422 (E1 and G1, red)) and anti-PHF-tau (AT8 and PHF-1) (H1 and I1, green) in AD brains. Scale bar is 120 μm for A1–2, B1–2, C1–2, 24 μm for A3, B3, C3, and 10 μm for D1–I2. Arrows indicate the co-localization. Immunostaining are representative from at least 3 independent experiments.

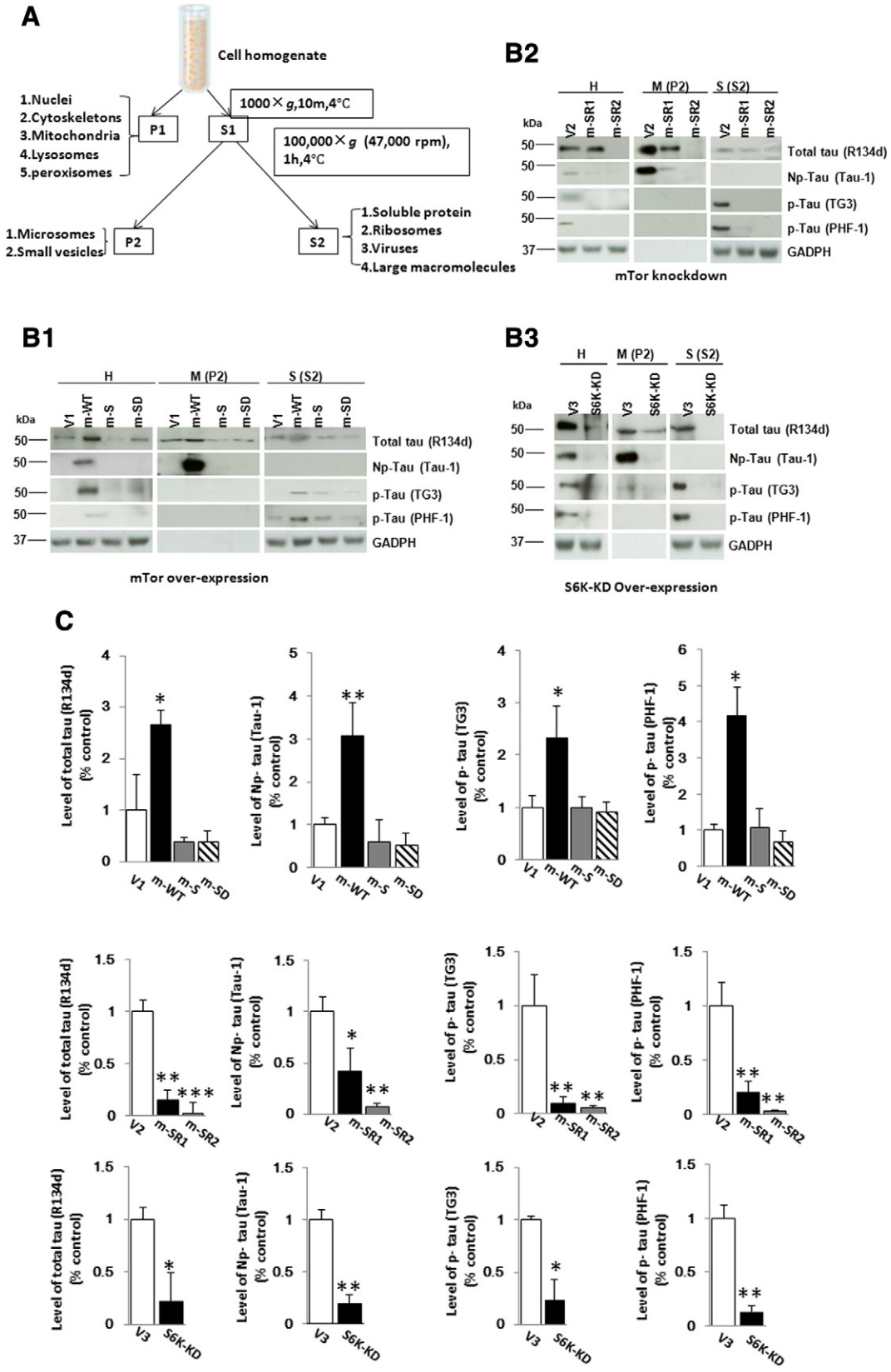

Fig. 2. Membrane and cytosolic fraction of Tau influenced by genetic interference of mTor activity. Panel A shows a schematic diagram of the cell fractionation procedure used for neuroblastoma cells to obtain membrane and cytosolic fractions. Panel B shows homogenate, membrane and cytosolic fraction of tau analyzed by Western blots: total (T), Non-phosphorylated (Np-) tau and phosphorylated (p) tau from three groups of human neuroblastoma cell lines transfected with 1) pcDNA3.0 (V1), flag wild type mTor (m-WT), flag mTor mutated at S2035T rapamycin resistant site (m-S), and mTor kinase dead mutated at both rapamycin resistant and activity sites (S2035T/D2357E, m-SD); 2) pLko.1 vector (V2), partial or complete silence of mTor by mTor shRNA1 (m-SR1) or mTor shRNA2 (m-SR2); 3) pcDNA3.0 and EECMV plasmids (V3), and S6K kinase dead (S6K-KD). Blots are representative from at least 3 independent experiments. The corresponding results from the independent experiments are presented as mean S.D.(error bars). *, $p < 0.05$; **, $p < 0.01$; ***, $p < 0.001$ compared with control.

3.3. mTor mediates localization and aggregation of tau in endoplasmic reticulum, mitochondria and Golgi apparatus

The synthesis, phosphorylation and aggregation of tau are also affected by mTor as we have shown in our previous study [26]. In order to determine whether mTor would influence the repartition of tau into different subcellular compartments, we have isolated ER, mitochondria and Golgi membrane fractions through differential and density gradient centrifugation from stable SH-SY5Y cellular models in which mTor activity was constitutively genetically modified

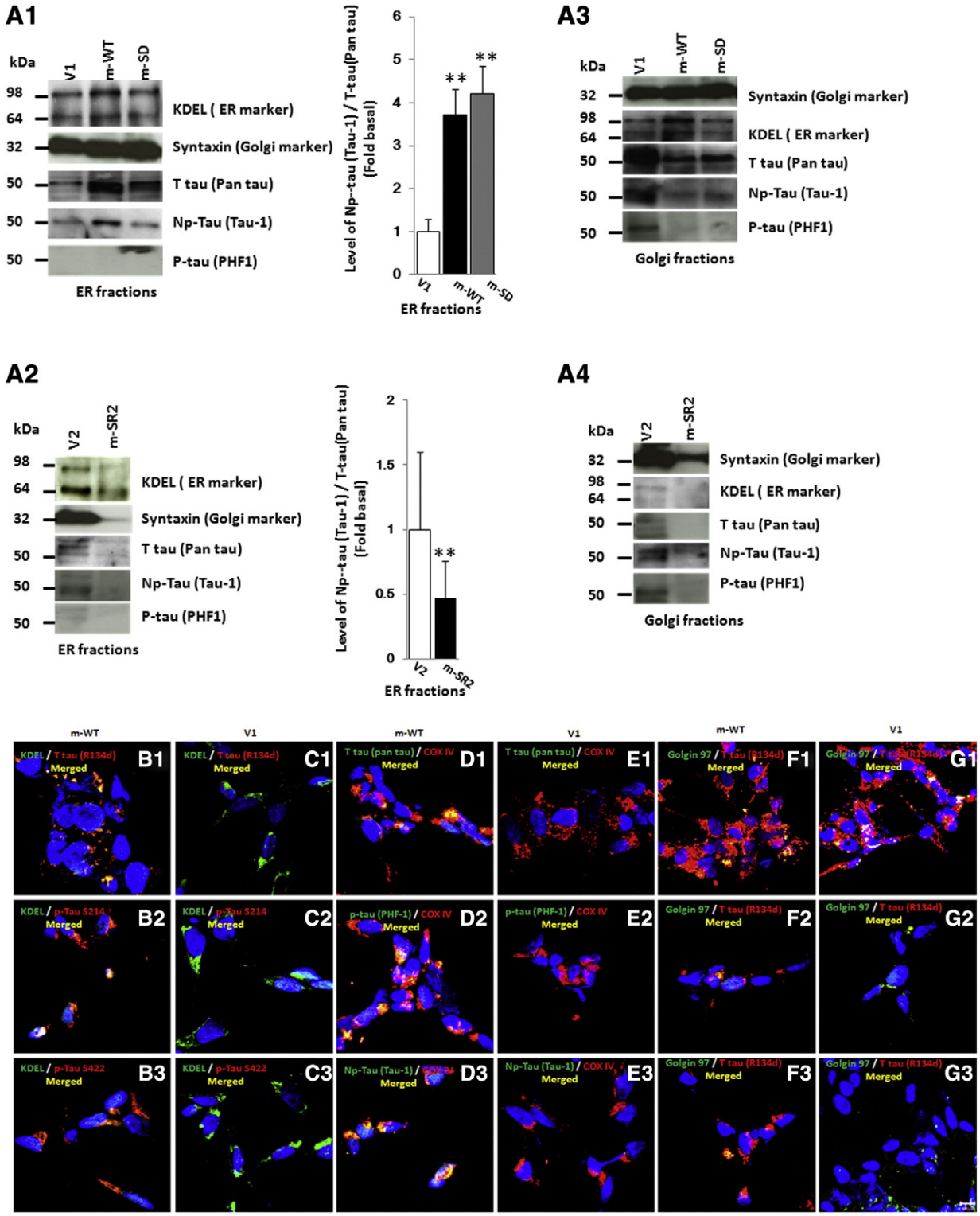

Fig. 3. Distribution of tau in different subcellular compartments in genetically modified mTor cells. Panel A shows Western blots of total tau (pan tau), Np-tau (Tau-1) and hyper-p-tau (PHF-1) from two groups of cell lines transfected with 1) pcDNA3.0 (V1), flag wild type mTor (m-WT), and mTor kinase dead mutated at both rapamycin resistant and activity sites (S2035T/D2357E, m-SD); 2) pLko.1 vector (V2), complete silence of mTor by mTor shRNA2 (m-SR2); Panels B–G show double immunostaining for T-tau, Np-tau and p-Tau and various subcellular markers KDEL (endoplasmic reticulum and cis-Golgi network marker) (B1–B3, C1–C3, green), COX IV (mitochondria marker) (D1–D3,E1–E3, red) and Golgin 97 (Golgi apparatus marker) (F1–F3, G1–G3, green) in V1 and m-WT. Scale bar is 10 μm. Immunostaining are representative from at least 3 independent experiments.

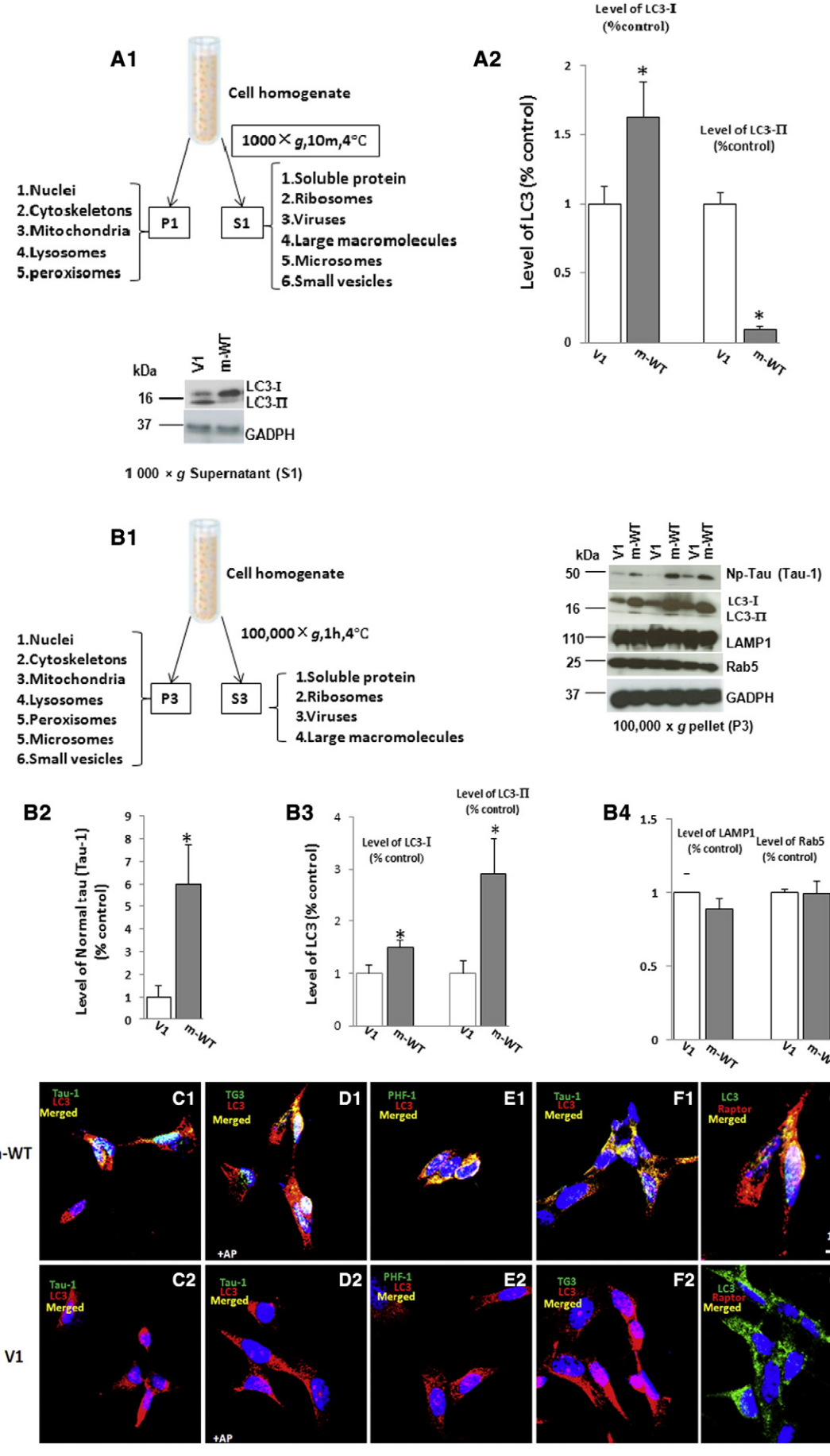
A1
Cell homogenate
1000× g,10m,4°C
1.Nuclei
2.Cytoskeletons
3.Mitochondria
4.Lysosomes
5.peroxisomes
P1
S1
1.Soluble protein
2.Ribosomes
3.Viruses
4.Large macromolecules
5.Microsomes
6.Small vesicles
kDa
V1
m-WT
16
LC3-I
LC3-II
37
GADPH
1 000 × g Supernatant (S1)
A2
Level of LC3-I (%control)
Level of LC3-II (%control)
Level of LC3 (% control)
B1
Cell homogenate
100,000× g,1h,4°C
1.Nuclei
2.Cytoskeletons
3.Mitochondria
4.Lysosomes
5.Peroxisomes
5.Microsomes
6.Small vesicles
P3
S3
1.Soluble protein
2.Ribosomes
3.Viruses
4.Large macromolecules
Np-Tau (Tau-1)
LAMP1
Rab5
100,000 x g pellet (P3)
B2
Level of Normal tau (Tau-1) (% control)
B3
Level of LC3-I (% control)
Level of LC3-II (% control)
Level of LC3 (% control)
B4
Level of LAMP1 (% control)
Level of Rab5 (% control)
m-WT
V1
C1
D1
E1
F1
G1
C2
D2
E2
F2
G2
Tau-1
TG3
PHF-1
LC3
Raptor
Merged
+AP
10μm

(Supplementary Fig. 1). KDEL (ER and cis-Golgi network marker) and syntaxin (Golgi apparatus marker) are used as marker proteins to identify ER or Golgi apparatus-containing fractions (Fig. 3B). Increased levels of total tau (pan tau) and Np-tau (Tau-1) but not p-tau (PHF-1) were detected in the ER fraction of m-WT compared with V1 and m-SD by Western blotting. Interestingly we have also found that down-regulation of mTor decreased the levels of total tau (pan tau) and Np-tau (Tau-1) in m-SR2 compared with V2. In Golgi fraction decreased immunoreactivity for total-, Np-, and p-tau could be detected in alignment with ER fractions possibly reflecting a deficiency in translation and trafficking of tau protein in mTor deficient cells. In pure mitochondrial fractions no tau species were detected by Western blot (data not showed). Since Golgi marker syntaxin showed a decreased immunoreactivity for total-, Np-, and p-tau in the Golgi fraction (Fig. 3A3), the increased extent of the levels of these anti-tau immunoreactivities in ER fraction stained by KDEL is less exposed since the KDEL also stained Golgi fraction (Fig. 3A1).

To further investigate whether the intracellular distribution of tau is altered by mTor in our cellular models we have cultured over-expressed wild type mTor (m-WT) and V1 control cells and deprived them of serum for 4.5 h in order to induce autophagy by inhibition of mTor activity, followed by immunostaining for a panel of tau antibodies and organelle markers. Immunostaining of KDEL (ER marker) has revealed an increased reactivity and localization with deposited tau (R134d, hyper-p-tau Ser(P)-422 and hyper-p-tau Ser(P)-214) in m-WT as compared with V1 empty vector (Fig. 3, B1–C3); interestingly total tau (pan tau), PHF-1 and Np-tau (Tau1) have been found to be present and co-localized with COXIV (mitochondria marker) mainly in m-WT (Fig. 3, D1–E3). In respect to the Golgin 97 immunostaining partial co-overlap was observed in m-WT as compared with V1 between the Golgi marker and deposited tau (R134d, hyper-p-tau Ser(P)-422 and hyper-p-tau Ser(P)-214) (Fig. 3, F1–G3).

3.4. Up-regulated mTor increases tau species in autophagic vacuoles

Next we explored the possibility if macroautophagy could be involved in intracellular accumulation of tau species and that AVs could present a site of tau accretion. In order to induce autophagic activity, m-WT and V1 cells were deprived of serum for 4.5 h, then the autophagic–lysosomal system was studied by ultracentrifugation, protein gel blotting and immunocytochemistry. Following a low speed centrifugation protocol at 1000 ×*g*, we have found that cells overexpressing mTor (m-WT) displayed decreased level of LC3–II when compared with V1 control cells in supernatant — S1 fraction (Fig. 4, A1–2) while the level of LC3-I has increased in m-WT. Interestingly, following higher speed centrifugation at 100,000 ×*g*, in membrane fraction (P3) containing lysosomes, peroxisomes, microsomes and other small vesicles, both Np- tau (Tau-1) and LC3 (LC3-I and LC3-II) immunoreactivity have dramatically increased in m-WT cell membrane fraction, while levels of Lamp1 (marker for lysosomes) and Rab5 (marker for early endosomes) were unchanged in both V1 and m-WT membrane fraction (Fig. 4, B1–4).

To further investigate the relationship between tau and autophagic vesicles, m-WT cells have been seeded and cultured on coverslips that were double stained for tau using Np-tau (Tau-1), p-tau (detection of alkaline phosphatase treated tau at S198/199/202/205 sites), and p-tau (PHF-1 and TG3) and AVs using LC3. Co-existence of tau with LC3 positive vacuoles was significantly more in m-WT cells compared with control V1 cells (Fig. 4, C1–F2). Of note, higher level of LC3 is detected in V1 control cells (Fig. 4, G2) with a decreased immunoreactivity for raptor compared with m-WT cells (Fig. 4, G1).

3.5. Up-regulated mTor increases the localization of intracellular tau within autophagic vacuoles and mediate its release in an exosome independent fashion

Both *in vitro* and *in vivo* data support the possibility that extracellular tau can be a key factor in tau pathology and its spreading [14,17,43]. Therefore we aimed to assess the extracellular tau protein found in conditioned media after serum deprivation of m-WT cells by analyzing dot blots for the presence of tau protein (Supplementary Fig. 2). Using Np-tau (Tau-1), p-tau (also for detection of alkaline phosphatase treated tau) and hyper-p-tau (PHF-1 and hyper-p-tau Ser(P)-214) antibodies to identify secreted tau species. Increased levels of tau species have been found in purified fractions (pellets 8) from conditioned culture media of m-WT cells compared to V1 controls. Regarding the levels of Tau-1 and hyper-p-tau (PHF-1 and hyper-p-tau Ser(P)-214) no significant changes could be detected between m-WT and V1 exosomal fractions (Fig. 5, A–B).

Immunogold labeling of m-WT and V1 cells with the NP-tau (Tau-1) antibody have shown that tau protein was localized with AVs and in close proximity to plasma membrane in m-WT cells (Fig. 5C). Thus Np-tau (Tau-1) immunogold labeling could suggest the association of Np-tau (Tau-1) with plasma membranes and its release from the cells (Fig. 5D). Taken together, the present data suggest that tau protein could be secreted by some exocytotic pathways in SH-SY5Y cells.

4. Discussion

The redistribution of p-tau from axons to somatodendrites and the defective tau traffic in subcellular compartments are considered as pathological markers during tauopathy development. Previously we found that mTor is involved in the translation, phosphorylation, and aggregation of tau in AD brains and SH-SY5Y cells containing different genetic modifications of mTor activity [26–28]. In the current study, we have focused on the alteration of tau protein in different cellular compartments responsible for protein translation, trafficking and secretion such as ER, Golgi apparatus and autophagosomes. A large number of studies, mostly in AD models, have explored the intracellular production sites of amyloid β (Aβ). Aβ40 and Aβ42 monomers are demonstrated in ER, trans-Golgi apparatus, post-trans-Golgi network secretory vesicles, autophagosomes, endosomes, lysosomes, multivesicular bodies, mitochondria, cytosol, and plasma membrane [44–50]. However subcellular localization of tau is less explored. In the present study, we have demonstrated that intracellular tau is partially localized to AVs, ER, mitochondria and Golgi apparatus in AD brains (Fig. 1). Overexpression of various mTor constructs in SH-SY5Y cells revealed increased levels of tau species, being partially co-localized with various subcellular compartments such as ER, mitochondrial or/and Golgi apparatus (Fig. 3). These results might indicate that up-regulated mTor mediates intracellular tau accumulation and plays a critical role in tau trafficking.

Both up-regulated mTor and S6K are associated with increased total tau in AD brains, and inhibition of mTor with rapamycin decreases the level of total tau both *in vitro* and *in vivo* [27,28,51,52]. Consistent with these findings, in the present study we have found that overexpression of mTor in human neuroblastoma cells leads to increased

Fig. 4. Up-regulated mTor increased tau accumulation in autophagic vacuoles. Representative Western blots in cell homogenates at 1000 ×*g* (A1–A2), analyzed with anti-LC3 antibodies; cell homogenates at 100,000 ×*g* (B1–B4) analyzed with anti-NP-tau (Tau-1), anti-LC3, anti-lamp1, anti-Rab5 antibodies in control cells (V1) and wild type mTor cells (m-WT). Anti-GADPH indicates loading control. Blots are representative from at least 3 independent experiments. The corresponding results from the independent experiments are presented as mean S.D. (error bars). *, $p < 0.05$ compared with control. C1–F2 show confocal microscopy of wild type mTor (m-WT) and control cells (V1) under serum deprivation for Np-tau (Tau-1, green), tau (Tau-1 antibody used for detection of alkaline dephosphatase treated tau, green) and hyper-p-tau (PHF-1 and TG3, green) co-localization with LC3 (red). G1 and G2 show immunostaining from control cells (V1) and wild type mTor cells (m-WT) with anti-LC3 (green) co-localization with raptor (red). Scale bar is 10 μm. Immunostaining is representative from at least 3 independent experiments.

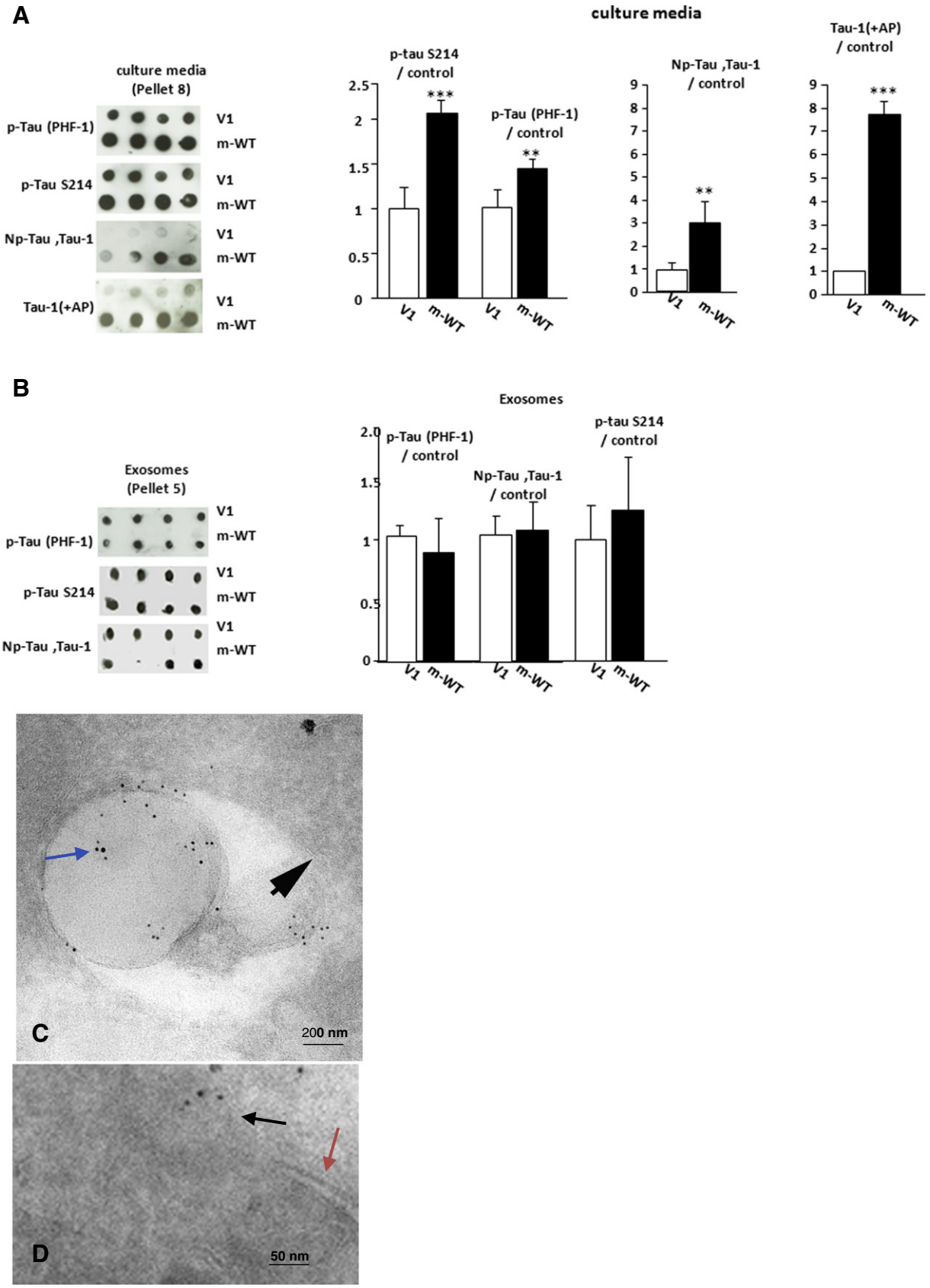

Fig. 5. Intracellular tau is localized to autophagic vacuoles and is released in association with non-exosome particles. Panels A and B show dot blotting with p-tau (PHF-1 and TG3), Np-tau (tau-1) and tau (tau-1 antibody used for detection of alkaline dephosphatase treated tau) from control cells (V1, 4 individual samples) and wild type mTor (m-WT, 4 individual samples) conditioned media. Panels C and D illustrate immunogold labeling of Np-tau (Tau-1) and its localization with autophagic vacuoles as well as proximity to the plasma membrane by immunoelectronic microscopy. Scale bar is 200 nm in C and 50 nm in D. Red arrow shows plasma membrane; black arrow—gold particles at the plasma membrane surface; blue arrow—gold particles in autophagic vacuoles; red arrow—plasma membrane; black arrow head—membrane with double layer of autophagic vacuoles.

total tau level, and overexpression of the inactive form of mTor, S6K or mTor silenced mutants decreases total tau (Fig. 2B). Tau phosphorylated at AD-specific sites TG3 (Thr231/Ser235) or PHF-1 (Ser396/404) could not be detected in neuronal membranes [10,53], but Np-tau (Ser199/202) was found to be associated with plasma membrane in transfected PC12 cells [54], or enriched in the membrane fraction of differentiated SH-SY5Y cells or tau transfected-non neural cos-1 cells [55]. It is the N-terminal half of tau that interacts with the plasma membrane in transfected PC12 cells [54]. In the present study, we have found that up-regulated mTor increases membrane-bound Np-tau (Tau-1) and cytosol-soluble p-tau (PHF-1 and TG3), and down-regulated mTor decreases membrane-bound Np-tau (Tau-1) and p-tau (PHF-1 and TG3) in cytosol (Fig. 2). Interestingly overexpression of mTor in SH-SY-5Y cell has been previously shown by us to suppress PP2A activity, the main tau phosphatase with concomitant increase in S6K phosphorylation at Thr 389 site and increase in GSK-3β phosphorylation at Ser9 site, contributing to increased tau phosphorylation at certain sites [26]. On the other hand, constitutive silencing of S6K (S6K-KD), the immediate downstream substrate of mTor, significantly decreased the level of tau phosphorylation. The increased level of membrane-bound Np-tau (Tau-1) in m-WT cells might also reflect newly synthesized tau.

The role of autophagy in AD is not well understood and contradicting reports have been published. For example, it has been reported that AVs may be a source of Aβ production and that AVs accumulate in AD brains and in the brains of APP/PS1 transgenic mice [34,56]. In contrast, other reports show that autophagy protects neurons from Aβ toxicity [57,58]. To complicate this apparent contradiction more, it has also been shown that mTor function, which negatively regulates autophagy, is increased in neurons that are predicted to develop tau pathology in AD brains, suggesting that high level of mTor signaling (and hence low level of autophagy) increases mTor gain-of-function occurred during aging, this process may facilitate the development of tau pathology [59,60].

Exocytosis has been implicated as a possible mechanism of amyloid spread as both prion and α-synuclein have been shown to be associated with exosomes in cultured cell media [61,62]. Tau was secreted and accumulated in membrane vesicles prepared from overexpressed tau kidney-derived cell lines culture medium [63,64]. Controversies exist since one study showed that tau is secreted by SH-SY5Y cells and tau in human CSF is associated with exosomes [65], other studies reported that tau was not detected in isolated exosomes from the neuroblastoma cells nor in primary mouse neuronal cultures [66–68]. In the present study, we have found no alteration among the tau species in the exosomes from control V1 compared to m-WT SH-SY5Y cells, however, increased levels of tau species have been found in pure protein extractions from conditioned culture medium of m-WT cells. Our present evidence indicates that up-regulated mTor facilitates the release of tau into extracellular space in an exosome independent fashion in SH-SY5Y cells, suggesting that mTor may mediate tau secretion by other alternative exosome free pathway.

In summary, considering a central role of mTor in the onset and progression of tau pathology in AD, our findings suggest that intracellular tau localized to various subcellular compartments is secreted to a large extent into extracellular space *via* an exosome independent manner. Our data also indicates that involvement of mTor in autophagic processing and secretion of tau could result in intracellular tau accumulation and its translocation to various cellular organelles as seen in AD brains and cellular models. These findings can provide a better understanding of the role of mTor in different tauopathies and could possibly contribute to development a novel therapeutics targeting mTor.

Abbreviations

AD	Alzheimer's disease
Akt	v-Akt murine thymoma viral oncogene homologue-1
AMPK	5′ adenosine monophosphate-activated protein kinase
AVs	autophagic vacuoles
Cdk5	cyclin-dependent protein kinases 5
DMEM	Dulbecco's modified eagle's medium
ER	endoplasmic reticulum
ERK1/2	extracellular signal-regulated kinase 1 and 2
NFT	neurofibrillary tangles
GSK-3β	glycogen synthase kinase-3β
m-WT	human flag-mTor wild type
m-S	human flag-mTor-S2035T (rapamycin resistant site)
m-SD	human flag-mTor-S2035T/D2357E (both rapamycin resistant and kinase dead sites)
m-SR	mTor shRNA
mTor	mammalian target of rapamycin
mTorC1	mTor Complex 1
mTorC2	mTor Complex 2
PDK	3-phosphoinositide dependent protein kinase
PHFs	pair helical filaments
PKA	cAMP-dependent protein kinase
S6K	p70 S6 kinase
S6K-KD	S6K kinase dead
SP	senile plaques
V1	selection empty pcDNA3.0 plasmids
V2	selection empty vector pLko.1
V3	both empty pcDNA3.0 vector and EECMV plasmids

Conflict of interest

This is to certify that there is no conflict of interest for all of the authors regarding the data presented in this manuscript.

Appendix A. Supplementary data

Supplementary data to this article can be found online at http://dx.doi.org/10.1016/j.bbamcr.2015.03.003.

References

[1] H. Braak, E. Braak, Frequency of stages of Alzheimer-related lesions in different age categories, Neurobiol. Aging 18 (1997) 351–357.
[2] T. Gomez-Isla, R. Hollister, H. West, S. Mui, J.H. Growdon, R.C. Petersen, J.E. Parisi, B.T. Hyman, Neuronal loss correlates with but exceeds neurofibrillary tangles in Alzheimer's disease, Ann. Neurol. 41 (1997) 17–24.
[3] A. Alonso, T. Zaidi, M. Novak, I. Grundke-Iqbal, K. Iqbal, Hyperphosphorylation induces self-assembly of tau into tangles of paired helical filaments/straight filaments, Proc. Natl. Acad. Sci. U. S. A. 98 (2001) 6923–6928.
[4] I. Grundke-Iqbal, K. Iqbal, Y.C. Tung, M. Quinlan, H.M. Wisniewski, L.I. Binder, Abnormal phosphorylation of the microtubule-associated protein tau (tau) in Alzheimer cytoskeletal pathology, Proc. Natl. Acad. Sci. U. S. A. 83 (1986) 4913–4917.
[5] H. Braak, E. Braak, I. Grundke-Iqbal, K. Iqbal, Occurrence of neuropil threads in the senile human brain and in Alzheimer's disease: a third location of paired helical filaments outside of neurofibrillary tangles and neuritic plaques, Neurosci. Lett. 65 (1986) 351–355.
[6] K. Iqbal, F. Liu, C.X. Gong, C. Alonso Adel, I. Grundke-Iqbal, Mechanisms of tau-induced neurodegeneration, Acta Neuropathol. 118 (2009) 53–69.
[7] J.Z. Wang, I. Grundke-Iqbal, K. Iqbal, Glycosylation of microtubule-associated protein tau: an abnormal posttranslational modification in Alzheimer's disease, Nat. Med. 2 (1996) 871–875.
[8] H. Braak, E. Braak, Neuropathological stageing of Alzheimer-related changes, Acta Neuropathol. 82 (1991) 239–259.
[9] B.T. Hyman, Tau propagation, different tau phenotypes, and prion-like properties of tau, Neuron 82 (2014) 1189–1190.
[10] A.M. Pooler, A. Usardi, C.J. Evans, K.L. Philpott, W. Noble, D.P. Hanger, Dynamic association of tau with neuronal membranes is regulated by phosphorylation, Neurobiol. Aging 33 (431) (2012) e427–e438.
[11] C.M. Waterman-Storer, J. Gregory, S.F. Parsons, E.D. Salmon, Membrane/microtubule tip attachment complexes (TACs) allow the assembly dynamics of plus ends to push and pull membranes into tubulovesicular networks in interphase Xenopus egg extracts, J. Cell Biol. 130 (1995) 1161–1169.
[12] C.A. Farah, S. Perreault, D. Liazoghli, M. Desjardins, A. Anton, M. Lauzon, J. Paiement, N. Leclerc, Tau interacts with Golgi membranes and mediates their association with microtubules, Cell Motil. Cytoskeleton 63 (2006) 710–724.
[13] W. Bondareff, C.Q. Mountjoy, M. Roth, D.L. Hauser, Neurofibrillary degeneration and neuronal loss in Alzheimer's disease, Neurobiol. Aging 10 (1989) 709–715.
[14] P. Cras, M.A. Smith, P.L. Richey, S.L. Siedlak, P. Mulvihill, G. Perry, Extracellular neurofibrillary tangles reflect neuronal loss and provide further evidence of

extensive protein cross-linking in Alzheimer disease, Acta Neuropathol. 89 (1995) 291–295.
[15] A.J. Green, R.J. Harvey, E.J. Thompson, M.N. Rossor, Increased tau in the cerebrospinal fluid of patients with frontotemporal dementia and Alzheimer's disease, Neurosci. Lett. 259 (1999) 133–135.
[16] M. Jensen, H. Basun, L. Lannfelt, Increased cerebrospinal fluid tau in patients with Alzheimer's disease, Neurosci. Lett. 186 (1995) 189–191.
[17] A. Gomez-Ramos, M. Diaz-Hernandez, R. Cuadros, F. Hernandez, J. Avila, Extracellular tau is toxic to neuronal cells, FEBS Lett. 580 (2006) 4842–4850.
[18] A. Gomez-Ramos, M. Diaz-Hernandez, A. Rubio, M.T. Miras-Portugal, J. Avila, Extracellular tau promotes intracellular calcium increase through M1 and M3 muscarinic receptors in neuronal cells, Mol. Cell. Neurosci. 37 (2008) 673–681.
[19] N.V. Mohamed, T. Herrou, V. Plouffe, N. Piperno, N. Leclerc, Spreading of tau pathology in Alzheimer's disease by cell-to-cell transmission, Eur. J. Neurosci. 37 (2013) 1939–1948.
[20] J.J. Pei, E. Braak, H. Braak, I. Grundke-Iqbal, K. Iqbal, B. Winblad, R.F. Cowburn, Distribution of active glycogen synthase kinase 3beta (GSK-3beta) in brains staged for Alzheimer disease neurofibrillary changes, J. Neuropathol. Exp. Neurol. 58 (1999) 1010–1019.
[21] J.J. Pei, H. Braak, W.L. An, B. Winblad, R.F. Cowburn, K. Iqbal, I. Grundke-Iqbal, Up-regulation of mitogen-activated protein kinases ERK1/2 and MEK1/2 is associated with the progression of neurofibrillary degeneration in Alzheimer's disease, brain research, Mol. Brain Res. 109 (2002) 45–55.
[22] J.J. Pei, S. Khatoon, W.L. An, M. Nordlinder, T. Tanaka, H. Braak, I. Tsujio, M. Takeda, I. Alafuzoff, B. Winblad, R.F. Cowburn, I. Grundke-Iqbal, K. Iqbal, Role of protein kinase B in Alzheimer's neurofibrillary pathology, Acta Neuropathol. 105 (2003) 381–392.
[23] J.Y. Chin, R.B. Knowles, A. Schneider, G. Drewes, E.M. Mandelkow, B.T. Hyman, Microtubule-affinity regulating kinase (MARK) is tightly associated with neurofibrillary tangles in Alzheimer brain: a fluorescence resonance energy transfer study, J. Neuropathol. Exp. Neurol. 59 (2000) 966–971.
[24] M. Laplante, D.M. Sabatini, mTOR signaling, Cold Spring Harb. Perspect. Biol. 4 (2012).
[25] M.G. Garelick, B.K. Kennedy, TOR on the brain, Exp. Gerontol. 46 (2011) 155–163.
[26] Z. Tang, E. Bereczki, H. Zhang, S. Wang, C. Li, X. Ji, R.M. Branca, J. Lehtio, Z. Guan, P. Filipcik, S. Xu, B. Winblad, J.J. Pei, Mammalian target of rapamycin (mTor) mediates tau protein dyshomeostasis: implication for Alzheimer disease, J. Biol. Chem. 288 (2013) 15556–15570.
[27] W.L. An, R.F. Cowburn, L. Li, H. Braak, I. Alafuzoff, K. Iqbal, I.G. Iqbal, B. Winblad, J.J. Pei, Up-regulation of phosphorylated/activated p70 S6 kinase and its relationship to neurofibrillary pathology in Alzheimer's disease, Am. J. Pathol. 163 (2003) 591–607.
[28] X. Li, I. Alafuzoff, H. Soininen, B. Winblad, J.J. Pei, Levels of mTOR and its downstream targets 4E-BP1, eEF2, and eEF2 kinase in relationships with tau in Alzheimer's disease brain, FEBS J. 272 (2005) 4211–4220.
[29] D.J. Klionsky, S.D. Emr, Autophagy as a regulated pathway of cellular degradation, Science 290 (2000) 1717–1721.
[30] S. Diaz-Troya, M.E. Perez-Perez, F.J. Florencio, J.L. Crespo, The role of TOR in autophagy regulation from yeast to plants and mammals, Autophagy 4 (2008) 851–865.
[31] N. Mizushima, H. Sugita, T. Yoshimori, Y. Ohsumi, A new protein conjugation system in human. The counterpart of the yeast Apg12p conjugation system essential for autophagy, J. Biol. Chem. 273 (1998) 33889–33892.
[32] Y. Kabeya, N. Mizushima, A. Yamamoto, S. Oshitani-Okamoto, Y. Ohsumi, T. Yoshimori, LC3, GABARAP and GATE16 localize to autophagosomal membrane depending on form-II formation, J. Cell Sci. 117 (2004) 2805–2812.
[33] A.M. Cuervo, E. Bergamini, U.T. Brunk, W. Droge, M. Ffrench, A. Terman, Autophagy and aging: the importance of maintaining "clean" cells, Autophagy 1 (2005) 131–140.
[34] W.H. Yu, A.M. Cuervo, A. Kumar, C.M. Peterhoff, S.D. Schmidt, J.H. Lee, P.S. Mohan, M. Mercken, M.R. Farmery, L.O. Tjernberg, Y. Jiang, K. Duff, Y. Uchiyama, J. Naslund, P.M. Mathews, A.M. Cataldo, R.A. Nixon, Macroautophagy—a novel Beta-amyloid peptide-generating pathway activated in Alzheimer's disease, J. Cell Biol. 171 (2005) 87–98.
[35] P. Bozidis, C.D. Williamson, A.M. Colberg-Poley, Isolation of endoplasmic reticulum, mitochondria, and mitochondria-associated membrane fractions from transfected cells and from human cytomegalovirus-infected primary fibroblasts, Juan S. Bonifacino, et al., (Eds.)Curr. Protoc. Cell Biol. (2007) 27 (Chapter 3, Unit 3).
[36] J.M. Graham, Isolation of Golgi membranes from tissues and cells by differential and density gradient centrifugation, Juan S. Bonifacino, et al., (Eds.)Curr. Protoc. Cell Biol. (2001) 9 (Chapter 3, Unit 3).
[37] C. Thery, S. Amigorena, G. Raposo, A. Clayton, Isolation and characterization of exosomes from cell culture supernatants and biological fluids, Curr. Protoc. Cell Biol. (2006) 22 (Chapter 3, Unit 3).
[38] F. Runau, L. Norris, J. Isherwood, M. Metcalfe, K. Brown, A.R. Dennison, Label-free proteomics: a potential method for identifying protein biomarkers in pancreatic cancer, Lancet 381 (2013) S96.
[39] J.A. Paulo, L.S. Lee, B.C. Wu, K. Repas, P.A. Banks, D.L. Conwell, H. Steen, Optimized sample preparation of endoscopic collected pancreatic fluid for SDS-PAGE analysis, Electrophoresis 31 (2010) 2377–2387.
[40] N. Haque, T. Tanaka, K. Iqbal, I. Grundke-Iqbal, Regulation of expression, phosphorylation and biological activity of tau during differentiation in SY5Y cells, Brain Res. 838 (1999) 69–77.
[41] K.T. Tokuyasu, A technique for ultracryotomy of cell suspensions and tissues, J. Cell Biol. 57 (1973) 551–565.
[42] A.S. Johansson, J.Z. Haeggstrom, K. Hultenby, J. Palmblad, Subcellular localization of leukotriene receptors in human endothelial cells, Exp. Cell Res. 316 (2010) 2790–2796.
[43] B. Frost, R.L. Jacks, M.I. Diamond, Propagation of tau misfolding from the outside to the inside of a cell, J. Biol. Chem. 284 (2009) 12845–12852.
[44] J.P. Greenfield, J. Tsai, G.K. Gouras, B. Hai, G. Thinakaran, F. Checler, S.S. Sisodia, P. Greengard, H. Xu, Endoplasmic reticulum and trans-Golgi network generate distinct populations of Alzheimer beta-amyloid peptides, Proc. Natl. Acad. Sci. U. S. A. 96 (1999) 742–747.
[45] K. Nishitsuji, T. Tomiyama, K. Ishibashi, K. Ito, R. Teraoka, M.P. Lambert, W.L. Klein, H. Mori, The E693Delta mutation in amyloid precursor protein increases intracellular accumulation of amyloid beta oligomers and causes endoplasmic reticulum stress-induced apoptosis in cultured cells, Am. J. Pathol. 174 (2009) 957–969.
[46] A.M. Cataldo, S. Petanceska, N.B. Terio, C.M. Peterhoff, R. Durham, M. Mercken, P.D. Mehta, J. Buxbaum, V. Haroutunian, R.A. Nixon, Abeta localization in abnormal endosomes: association with earliest Abeta elevations in AD and Down syndrome, Neurobiol. Aging 25 (2004) 1263–1272.
[47] C.A. Hansson Petersen, N. Alikhani, H. Behbahani, B. Wiehager, P.F. Pavlov, I. Alafuzoff, V. Leinonen, A. Ito, B. Winblad, E. Glaser, M. Ankarcrona, The amyloid beta-peptide is imported into mitochondria via the TOM import machinery and localized to mitochondrial cristae, Proc. Natl. Acad. Sci. U. S. A. 105 (2008) 13145–13150.
[48] G.K. Gouras, J. Tsai, J. Naslund, B. Vincent, M. Edgar, F. Checler, J.P. Greenfield, V. Haroutunian, J.D. Buxbaum, H. Xu, P. Greengard, N.R. Relkin, Intraneuronal Abeta42 accumulation in human brain, Am. J. Pathol. 156 (2000) 15–20.
[49] J.H. Chyung, D.M. Raper, D.J. Selkoe, Gamma-secretase exists on the plasma membrane as an intact complex that accepts substrates and effects intramembrane cleavage, J. Biol. Chem. 280 (2005) 4383–4392.
[50] R.H. Takahashi, T.A. Milner, F. Li, E.E. Nam, M.A. Edgar, H. Yamaguchi, M.F. Beal, H. Xu, P. Greengard, G.K. Gouras, Intraneuronal Alzheimer abeta42 accumulates in multivesicular bodies and is associated with synaptic pathology, Am. J. Pathol. 161 (2002) 1869–1879.
[51] J.J. Pei, W.L. An, X.W. Zhou, T. Nishimura, J. Norberg, E. Benedikz, J. Gotz, B. Winblad, P70 S6 kinase mediates tau phosphorylation and synthesis, FEBS Lett. 580 (2006) 107–114.
[52] M.S. Caccamo, A. Richardson, R. Strong, S. Oddo, Molecular interplay between mammalian target of rapamycin (mTOR), amyloid-beta, and Tau: effects on cognitive impairments, J. Biol. Chem. 285 (2010) 13107–13120.
[53] T. Maas, J. Eidenmuller, R. Brandt, Interaction of tau with the neural membrane cortex is regulated by phosphorylation at sites that are modified in paired helical filaments, J. Biol. Chem. 275 (2000) 15733–15740.
[54] R. Brandt, J. Leger, G. Lee, Interaction of tau with the neural plasma membrane mediated by tau's amino-terminal projection domain, J. Cell Biol. 131 (1995) 1327–1340.
[55] M. Arrasate, M. Perez, J. Avila, Tau dephosphorylation at tau-1 site correlates with its association to cell membrane, Neurochem. Res. 25 (2000) 43–50.
[56] B. Boland, A. Kumar, S. Lee, F.M. Platt, J. Wegiel, W.H. Yu, R.A. Nixon, Autophagy induction and autophagosome clearance in neurons: relationship to autophagic pathology in Alzheimer's disease, J. Neurosci. 28 (2008) 6926–6937.
[57] D. Ling, P.M. Salvaterra, A central role for autophagy in Alzheimer-type neurodegeneration, Autophagy 5 (2009) 738–740.
[58] D. Ling, H.J. Song, D. Garza, T.P. Neufeld, P.M. Salvaterra, Abeta42-induced neurodegeneration via an age-dependent autophagic-lysosomal injury in Drosophila, PLoS One 4 (2009) e4201.
[59] J.J. Pei, J. Hugon, mTOR-dependent signalling in Alzheimer's disease, J. Cell. Mol. Med. 12 (2008) 2525–2532.
[60] S. Oddo, The role of mTOR signaling in Alzheimer disease, Front. Biosci. 4 (2012) 941–952.
[61] B. Fevrier, D. Vilette, F. Archer, D. Loew, W. Faigle, M. Vidal, H. Laude, G. Raposo, Cells release prions in association with exosomes, Proc. Natl. Acad. Sci. U. S. A. 101 (2004) 9683–9688.
[62] E. Emmanouilidou, L. Stefanis, K. Vekrellis, Cell-produced alpha-synuclein oligomers are targeted to, and impair, the 26S proteasome, Neurobiol. Aging 31 (2010) 953–968.
[63] D. Simon, E. Garcia-Garcia, A. Gomez-Ramos, J.M. Falcon-Perez, M. Diaz-Hernandez, F. Hernandez, J. Avila, Tau overexpression results in its secretion via membrane vesicles, Neurodegener. Dis. 10 (2012) 73–75.
[64] D. Simon, E. Garcia-Garcia, F. Royo, J.M. Falcon-Perez, J. Avila, Proteostasis of tau. Tau overexpression results in its secretion via membrane vesicles, FEBS Lett. 586 (2012) 47–54.
[65] S. Saman, W. Kim, M. Raya, Y. Visnick, S. Miro, S. Saman, B. Jackson, A.C. McKee, V.E. Alvarez, N.C. Lee, G.F. Hall, Exosome-associated tau is secreted in tauopathy models and is selectively phosphorylated in cerebrospinal fluid in early Alzheimer disease, J. Biol. Chem. 287 (2012) 3842–3849.
[66] J. Faure, G. Lachenal, M. Court, J. Hirrlinger, C. Chatellard-Causse, B. Blot, J. Grange, G. Schoehn, Y. Goldberg, V. Boyer, F. Kirchhoff, G. Raposo, J. Garin, R. Sadoul, Exosomes are released by cultured cortical neurones, Mol. Cell. Neurosci. 31 (2006) 642–648.
[67] I. Santa-Maria, M. Varghese, H. Ksiezak-Reding, A. Dzhun, J. Wang, G.M. Pasinetti, Paired helical filaments from Alzheimer disease brain induce intracellular accumulation of tau protein in aggresomes, J. Biol. Chem. 287 (2012) 20522–20533.
[68] C.M. Karch, A.T. Jeng, A.M. Goate, Extracellular tau levels are influenced by variability in tau that is associated with tauopathies, J. Biol. Chem. 287 (2012) 42751–42762.